Cosmic ray $e^{\pm}$ at high energy

Kfir Blum[1,2,*] and *Annika* Reinert[3,**]

[1]Department of Particle Physics & Astrophysics, Weizmann Institute of Science, Rehovot, Israel
[2]CERN Theory Department
[3]Bethe Center for Theoretical Physics and Physikalisches Institut der Universität Bonn, Nußallee 12, 53115 Bonn, Germany

Abstract. There is a commonly expressed opinion in the literature, that cosmic-ray (CR) e^+ come from a primary source, which could be dark matter or pulsars. In these *proceedings* we review some evidence to the contrary: namely, that e^+ come from secondary production due to CR nuclei scattering on interstellar matter. We show that recent measurements of the total $e^{\pm}$ flux at $E \gtrsim 3$ TeV are in good agreement with the predicted flux of secondary $e^{\pm}$, that would be obtained if radiative energy losses during CR propagation do not play an important role. If the agreement between data and secondary prediction is not accidental, then the requirement of negligible radiative energy losses implies a very short propagation time for high energy CRs: $t_{\rm esc} \lesssim 10^5$ yr at rigidities $\mathcal{R} \gtrsim 3$ TV. Such short propagation history may imply that a recent, near-by source dominates the CRs at these energies. We review independent evidence for a transition in CR propagation, based on the spectral hardening of primary and secondary nuclei around $\mathcal{R} \sim 100$ GV. The transition rigidity of the nuclei matches the rigidity at which the e^+ flux saturates its secondary upper bound.

1 CR $e^{\pm}$ at $E \sim 3$ TeV saturate the secondary upper bound

Measurements of Galactic CR in the energy range (1 – 10^4) GeV have improved significantly in the last decade. For $e^{\pm}$, in particular, the individual fluxes of e^+ and e^- up to $\sim$ 1 TeV and the total $e^{\pm}$ flux up to $\sim$ 10 TeV became available thanks to the PAMELA [1], AMS02 [2], DAMPE [3], CALET [4, 5], Fermi-LAT [6], HESS [7, 8], VERITAS [9], and MAGIC [10] experiments. Some of the key measurements are summarised in Fig. 1. (At TeV energies, $e^{\pm}$ data sets from AMS02 [2] and CALET [5], on the one hand, and from DAMPE [3], Fermi-LAT [6], and HESS [7, 8], on the other hand, are not fully consistent, indicating systematic errors. This current disagreement on the details of the flux does not affect our discussion.)

Fig. 1 shows measurements of the total $e^{\pm}$ flux by DAMPE [3] (blue markers) and HESS (green), as well as measurements of the individual flux of e^+ by AMS02 [2] (red). Preliminary measurements by AMS02, extending to higher energy, are also shown [11] (brown). The e^+ flux in Fig. 1 is shown multiplied by a factor of 2: we'll explain the reason for this presentation shortly.

It is well known, and obvious from Fig. 1, that e^- and e^+ below $\sim$ 1 TeV come from separate sources: the e^- flux (and thus the total $e^{\pm}$ flux) is larger than the e^+ flux by a factor of $O(10)$. The bulk of the e^- flux in this energy range is thought to be primary, due to Fermi acceleration of ambient ISM e^- at astrophysical shocks. In contrast, the origin of e^+ is not known. There are suggestions that e^+ are produced by exotic primary sources like dark matter annihilation (see, e.g. [12–15]) or pulsars (see, e.g. [16–19]). Alternatively, the e^+ may be due to secondary production in CR nuclei collisions with ISM [20].

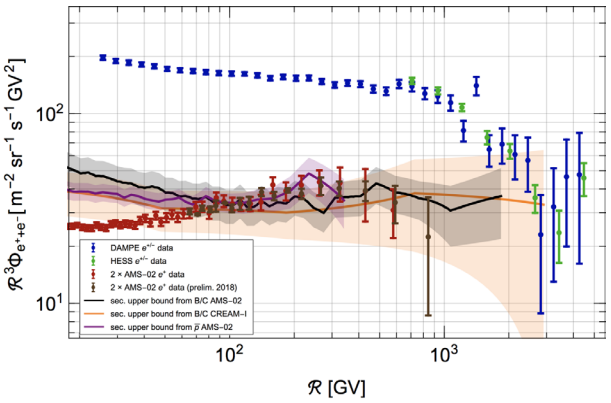

Figure 1. $e^{\pm}$ data from DAMPE [3] (blue) and HESS (green), and (**2**×) e^+ data from AMS02 [2] (red), compared with the secondary $e^{\pm}$ upper bound derived from AMS02 B/C (black), CREAM-I B/C (orange), and AMS02 $\bar{p}$ (purple).

There is (we think) an important hint in the data, that supports a secondary origin for e^+. To see this, in Fig. 1 we supplement the experimental data with a theory calculation, shown by the shaded bands. The calculation shows the secondary flux of e^+ that would be predicted if radiative energy losses of e^+, during the propagation from the production point to the Earth, are not important. If we "turn off" radiative losses, then the propagation problem for secondary e^+ becomes similar to that for other sec-

*e-mail: kfir.blum@cern.ch
**e-mail: areinert@th.physik.uni-bonn.de

ondary CR nuclei, like B and $\bar{p}$. We can use the measured fluxes of B or $\bar{p}$ to calibrate out the effect of propagation, and predict the (no-loss) flux of secondary e^+ using known production and fragmentation cross sections. Thanks to progress at the LHC and other high-energy accelerator experiments, the most important cross sections are now directly calibrated against data, up to multi-TeV e^+ energies [21][1].

The answer that we get by "turning off" energy losses, is an upper bound to the flux of secondary e^+ [20]. In Fig. 1, the black shaded band shows the result obtained when using B and other nuclei data from AMS02 to calibrate out the propagation. The orange band shows the result of the same exercise, but this time using B/C data from CREAM that extends to higher rigidity. The purple band shows the result of a similar exercise, using $\bar{p}$ data from AMS02. This last calculation is the most robust one, because secondary $\bar{p}$ and e^+ come from the same secondary production mechanism (mostly p and He collisions with ISM) while B comes from fragmentation of heavier nuclei (mostly C and O), involving different systematic uncertainties.

The measured e^+ flux in Fig. 1 saturates the secondary e^+ flux upper bound [23]. It may be useful to note that the upper bound was predicted in Ref. [20] before high energy e^+ data at $E > 100$ GeV became available. If e^+ are in fact primary, from e.g. pulsars, then this saturation of the secondary bound is an accidental coincidence[2][3]. We cannot rule out such accidental coincidence. However, we think that the saturation of the secondary bound is a strong motivation to consider the hypothesis that e^+ are, well, secondary. The theoretical challenge that follows, in this case, is to explain what CR propagation scenario, if any, could result with ineffective radiative energy losses for secondary e^+.

The recent high-energy $e^\pm$ data in Fig. 1, extending to $E \sim 5$ TeV, suggest a new coincidence. As discussed above, CR e^- at $E < 1$ TeV are primary. At $E \gtrsim 1$ TeV, however, the data show that the $e^\pm$ flux falls off, in what may be a radiative cooling cut-off (of the primary e^- component, possibly occurring at the e^- acceleration site.) The point we wish to note here is that at yet higher energy, $E \gtrsim 3$ TeV, the flux fall-off appears to cease. Interestingly, the flux at $E \gtrsim 3$ TeV saturates to a value that is, once again, consistent with the secondary flux upper bound. It is for this reason – to compare the secondary upper bound prediction with the total $e^\pm$ measured flux – that we have shown the e^+ flux multiplied by a factor of 2. High-energy secondary production of e^+ predicts an almost equal flux of secondary e^- [21].

We think that the $E \gtrsim 3$ TeV saturation of the measured $e^\pm$ flux with the secondary bound, is new evidence in favour of the secondary source hypothesis for e^+ (and, at these energies, e^-). This interpretation reinforces the theoretical challenge, of explaining why radiative energy losses do not affect the flux of secondary $e^\pm$. The only way to achieve this, is by a short propagation time for TV secondary CR: shorter than the radiative cooling time of TeV $e^\pm$. In the next section we discuss this possibility.

We note that a more direct check of secondary multi-TeV $e^\pm$, would be achieved by measuring the $e^+/e^\pm$ ratio at these energies. If our interpretation is correct, then $e^+/e^- \approx 1$ at $E = 3$ TeV.

2 Secondary $e^\pm$ at $E \sim 3$ TeV require (very?) short propagation time

How could CR $e^\pm$ at $E \gtrsim 3$ TeV, not be significantly affected by radiative energy losses during the propagation? The most commonly adopted steady-state diffusion models of CR propagation [25] predict, to the contrary, that energy losses should completely dominate the behaviour of the secondary $e^\pm$ flux at these energies.

Radiative losses become ineffective if the CR propagation time-scale, $t_{\rm esc}$, is shorter than the $e^\pm$ radiative loss time-scale, $t_{\rm cool}$ [20]. It is important to note, that the widely used diffusion models for CR propagation have been successfully tested and calibrated along the years to fit observations of stable nuclei. These nuclei data include a zoo of different elements, from primary p, He, C, O, Fe,... to secondary B, Li, sub-Fe (that is, the Sc-Ti-V-Cr group), and recently $\bar{p}$. CR nuclei test the amount of nuclear transformation undergone by CR during propagation. This constrains the column density of target material traversed along the CR path. Stable nuclei data are not, however, sensitive to the *time* it takes the CR to traverse that column density. Traditionally, CR models attempted to overcome this ambiguity about propagation time by adjusting the models to fit low-energy secondary radioactive isotopes (notably ^{10}Be), and some scarce radioactive-sensitive elemental data (notably the Be/B ratio) [20, 26, 27]. The first class of measurements (^{10}Be) does not help us much: it only extends to $\mathcal{R} \lesssim 1$ GV, while the riddle we face with the $e^\pm$ appears at $\mathcal{R} \gtrsim 100$ GV. The second class of measurements (Be/B) provides useful constraints up to $\mathcal{R} \sim 20$ GV, however (i) it is strongly affected by systematic uncertainties of fragmentation cross sections, and (ii) it does not provide additional information at $\mathcal{R} \gtrsim 30$ GV, because the Lorentz-dilated observer frame lifetime of ^{10}Be, $t_{\rm d} \approx 20\,(\mathcal{R}/20\ {\rm GV})$ Myr, becomes much longer than the CR propagation time so that Be becomes just another effectively-stable secondary, like B. Lastly, we note that recent Be/B measurements by AMS02 [28] are not fully consistent with earlier measurements by HEAO3 [29], although the two experiments have

[1] Nevertheless, we note that this calibration is incomplete because existing LHC data does not probe the entire kinematical region relevant for CR secondary production: high-rapidity measurements are missing. There is ongoing effort to supplement the missing data at the LHC, by arranging for a fixed-target experimental set-up [22].

[2] See discussion in [24], and the pulsar example in Fig. 15 there.

[3] There is another point to be made here. In computing the shaded bands in Fig. 1, there are, of course, statistical measurement and systematic flux and cross section uncertainties, reflected by the width of the band. However, *there are no free theoretical model parameters*. This must be contrasted with, e.g., pulsar models for CR e^+, where free parameters of the model are adjusted to fit the e^+ injection efficiency and spectrum, and the unknown details of the propagation from the pulsar to Earth (which cannot be calibrated out using any other CR species, because the pulsar is postulated to produce only $e^\pm$), in order to match the measured e^+ flux.

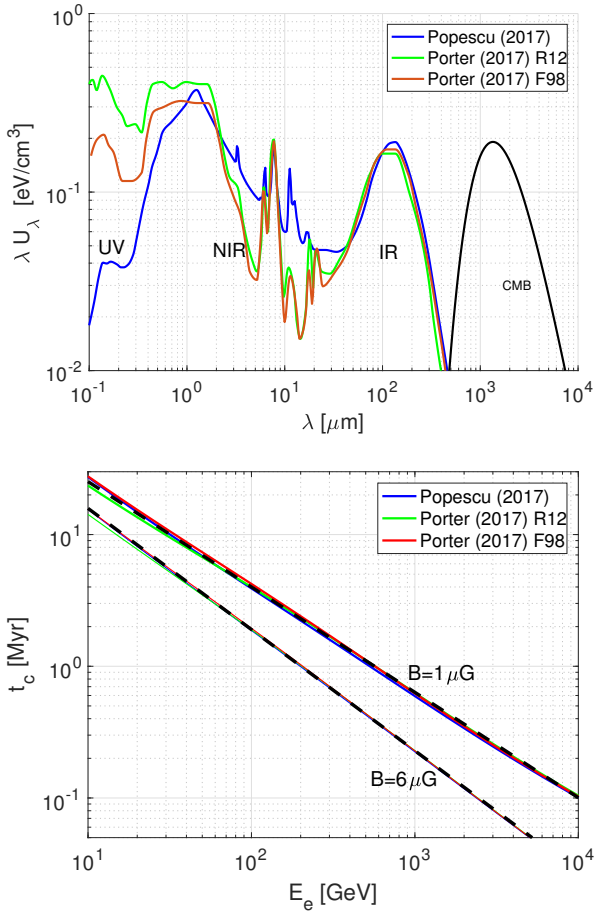

Figure 2. Upper panel: ISRF models. **Lower panel:** $e^{\pm}$ cooling time vs. energy, for three ISRF models [31, 32]. Upper dashed line shows $4\,(\mathcal{R}/100\ \mathrm{GV})^{-0.8}$, lower dashed line shows $1.9\,(\mathcal{R}/100\ \mathrm{GV})^{-0.92}$.

comparable nominal precision for this particular observable.

In short, the e^+ and $e^{\pm}$ data itself is, to date, the only probe of the CR propagation time that is currently available at high energies, $\mathcal{R} \gtrsim 100$ GV. If we take it from Fig. 1 that at $\mathcal{R} \gtrsim 3$ TV, $e^{\pm}$ are secondary, then given an estimate of the effective $e^{\pm}$ cooling time at these energies, $t_{\rm cool}$, we can deduce an upper bound $t_{\rm esc} < t_{\rm cool}$. The cooling time can be calculated given an estimate of the interstellar radiation field (ISRF) and magnetic fields in the propagation region [30]. In the upper panel of Fig. 2 we show three ISRF models, taken from recent literature [31, 32]. In the lower panel we show the radiative cooling time $t_{\rm cool}$ computed using these ISRF models. In addition to the ISRF, we add magnetic field $B = 1\ \mu$G (upper set of lines) and $6\ \mu$G (lower lines, difficult to resolve by eye). This range of B roughly spans the expectations for the real situation in an average region in the Galaxy. The upper dashed line[4] in the lower panel of Fig. 2 shows $4\,(\mathcal{R}/100\ \mathrm{GV})^{-0.8}$. The lower dashed line shows $1.9\,(\mathcal{R}/100\ \mathrm{GV})^{-0.92}$.

[4]We note that with the ISRF parametrisations of [31, 32], we do not find room for pronounced Klein-Nishina steps [33].

The $e^{\pm}$ cooling time deduced from Fig. 2 is $t_{\rm cool}(3\ \mathrm{TV}) \sim (0.1-0.3)$ Myr. This gives an upper limit for the CR propagation time, that we take to be, roughly,

$$t_{\rm esc}(\mathcal{R} = 3\ \mathrm{TV}) \lesssim 0.1\ \mathrm{Myr}. \quad (1)$$

How far off is Eq. (1), compared to the expectations from steady-state diffusion models? With commonly adopted values for the parameters of these models, a diffusion coefficient of $D \approx 4 \times 10^{28}\,(\mathcal{R}/1\ \mathrm{GV})^{0.4}$ cm^2/sec, and a CR halo scale height of $L \approx 5$ kpc, the escape time in the diffusion model, $t_{\rm esc}^{\rm diff} = L^2/(2D)$, is expected to be $t_{\rm esc}^{\rm diff}(\mathcal{R} = 3\ \mathrm{TV}) \sim 10$ Myr, a factor of ~ 100 longer than is permitted by Eq. (1). Either the diffusion model is wrong, or else the $e^{\pm}$ are not secondary. The contradiction remains also if we consider only the lower energy e^+, at $\mathcal{R} \sim 300$ GV, to be secondary. Here the discrepancy between the upper bound on $t_{\rm esc}$ and the value expected in the diffusion model is about a factor of 10. If we go down further to $\mathcal{R} = 10$ GV, the diffusion model predicts $t_{\rm esc}^{\rm diff}(\mathcal{R} \sim 10\ \mathrm{GV}) \sim 100$ Myr, while the cooling time is $t_{\rm cool}(\mathcal{R} \sim 10\ \mathrm{GV}) \sim (10-30)$ Myr. When energy loss is dominant, the diffusion model makes a generic prediction for the suppression of the flux. Parametrising the suppression by $f_e = J_{e^+}/J_{e^+}^{\rm no-loss}$, the diffusion model predicts $f_e^{\rm diff} \approx 0.8\sqrt{t_{\rm cool}/t_{\rm esc}}$, which gives $f_e^{\rm diff}(\mathcal{R} = 10\ \mathrm{GV}) \approx (0.25-0.5)$. Inspecting the data vs. upper bound at $\mathcal{R} = 10$ GV in Fig. 1, the e^+ data does hint for some suppression of the flux, which is in fact consistent with the diffusion model expectation.

3 Coincident trends in nuclei and e^+

It is illuminating to inspect the behaviour of e^+ alongside the behaviour of secondary nuclei. In Fig. 3, in the upper panel, we plot the measured e^+ flux divided by the theoretical secondary e^+ upper bound. We denote this ratio by $f_e^{\rm obs}$. Note that in this calculation, we use $\bar{p}$ data to extract f_e directly, without reference to nuclei data. In the lower panel we plot $X_{\rm esc}$, calculated from nuclei data, scaled by a factor of $\mathcal{R}^{\zeta}$ with $\zeta = 0.55$, to highlight the spectral shape. As noted before, the e^+ flux rises to and saturates the secondary upper bound, signified by $f_e^{\rm obs} = 1$. The saturation rigidity of $f_e^{\rm obs}$, $\mathcal{R} \sim 100$ GV, is close to a hardening break seen in $X_{\rm esc}$: at $\mathcal{R} \gtrsim 100$ GV, the spectral index of $X_{\rm esc}$ is hardened by $\Delta\zeta \approx 0.2$. This is highlighted by the dashed line. The spectral hardening, that we exhibit here in terms of the CR grammage, is consistent with recent analyses by the AMS02 collaboration [28] (see also [34, 35]).

4 Discussion and summary

We have presented some new evidence, supporting the possibility that CR e^+ are dominantly coming from secondary production:

1. As shown in Fig. 1, measurements of the $e^{\pm}$ flux at $E \sim 3$ TeV are consistent with the flux expected from secondary production, if radiative energy losses during secondary $e^{\pm}$ propagation are not

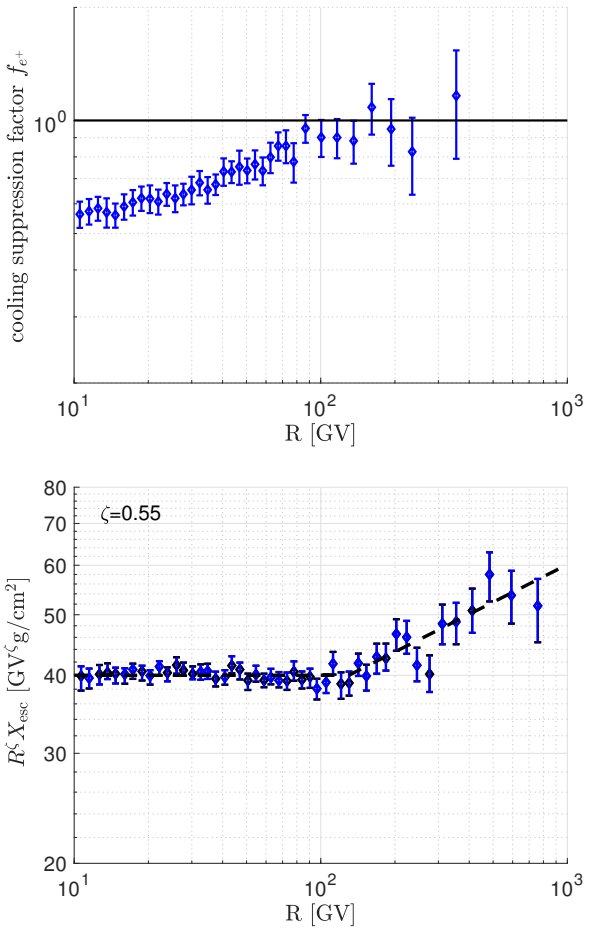

Figure 3. Upper: e^+ cooling suppression factor, derived from e^+ and $\bar{p}$ data. **Lower:** CR grammage, derived from nuclei data. The dashed line highlights the hardening break in $X_{\rm esc}$. It starts at $\mathcal{R}$ = 130 GV with slope $\mathcal{R}^{0.2}$.

important. This coincidence with the secondary flux adds to the earlier observation, that the e^+ flux in the range $E \sim 100-800$ TeV saturates the no-loss upper bound. We note that direct parametrisation of LHC data, necessary for the calculation of secondary $e^\pm$ production at multi-TeV energies, have now become available [21].

2. As shown in Fig. 3, the transition of the e^+ data, into saturating the secondary upper bound, occurs at $\mathcal{R} \sim 100$ GV and is correlated with another observed transition in the CR grammage $X_{\rm esc}$, measured for secondary nuclei B, Li, and Be.

Interpreting Fig. 1 to imply that e^+ are secondary in the entire measured energy range $E \sim (10 - 10^4)$ GeV, we would deduce that the propagation time of CR satisfies $t_{\rm esc}(\mathcal{R} = 10\ {\rm GV}) \gtrsim 10$ Myr (based on the hint for $O(1)$ suppression of the e^+ flux at this energy), and $t_{\rm esc}(\mathcal{R} = 3\ {\rm TV}) \lesssim 0.1$ Myr (based on the hint for negligible effect of loss). Thus, $t_{\rm esc}$ must decrease fast with $\mathcal{R}$. If the propagation time was a smooth power-law in rigidity, $t_{\rm esc} \propto \mathcal{R}^{-\alpha}$, then we must deduce $\alpha \gtrsim 0.8$. (More precisely, the requirement is, roughly, $t_{\rm esc} \lesssim t_{\rm cool}$ for $\mathcal{R} \gtrsim 100$ GV. In the Thomson limit one has $t_{\rm cool} \propto \mathcal{R}^{-1}$. However, KN corrections due to the UV component in the ISRF lead to $t_{\rm cool} \sim \mathcal{R}^{-\alpha_c}$, with $\alpha_c \sim 0.8$ in the energy range of interest.) This possibility was considered in [20][5]. However, a smooth power-law model for $t_{\rm esc}$ must give over to another behaviour at yet higher rigidity, probably by $\mathcal{R} \sim 100$ TV or so. The reason is that accepting power-law $t_{\rm esc}$ all the way to very high rigidities, with $\alpha \gtrsim 0.8$, we would be led to $t_{\rm esc}(\mathcal{R} = 500\ {\rm TV}) \lesssim 2$ kyr. This is an unacceptably small value for $t_{\rm esc}$: if there were a CR source near Earth in the last 2 kyr, we would see it.

Another possibility is that CRs in the range between few GV to few TV, are not well described by some global, smooth power-law propagation history. Instead, it may be the case that we are seeing transitions between different populations of CR sources, with an older population of sources, characterised by $t_{\rm esc} \gtrsim 10$ Myr, dominating the CRs below $\mathcal{R} \sim 10$ GV, and other sources, possibly a single source characterised by $t_{\rm esc} \sim 0.1$ Myr, dominating the flux above $\mathcal{R} \sim 100$ GV.

Either way, with a short propagation time of ~ 0.1 kyr, we expect to see structure in the CR flux, reflecting a transition between different populations of sources or different mechanisms of CR propagation. Proton and helium measurements, extending from sub-TV up to several PV [36] (see [37] for a recent review of relevant measurements), do not seem inconsistent with such transitions, in the sense that the data does not appear to be well described by a simple power-law but rather suggests a certain degree of structure.

Acknowledgements

We are grateful to Boaz Katz, Kohta Murase, and Eli Waxman for many useful discussions, and to the organisers of ISVHECRI 2018 (Nagoya U.) for a very productive conference. The idea, of calculating the flux of secondary e^+ without radiative losses and using it as an upper bound, is originally due to Boaz Katz. The work in these proceedings will appear in a separate paper containing further analysis and results. KB was supported by grant 1937/12 from the I-CORE program of the Planning and Budgeting Committee and the Israel Science Foundation and by grant 1507/16 from the Israel Science Foundation, and is incumbent of the Dewey David Stone and Harry Levine career development chair.

References

[1] O. Adriani et al. (PAMELA), Nature **458**, 607 (2009), 0810.4995
[2] M. Aguilar et al. (AMS), Phys. Rev. Lett. **113**, 221102 (2014)
[3] G. Ambrosi et al. (DAMPE), Nature **552**, 63 (2017), 1711.10981

[5] In [20] it was also noted that to accommodate B/C data, which constrains the CR grammage to follow $X_{\rm esc} \propto \mathcal{R}^\delta$ with $\delta \approx 0.4$, the characteristic scale height of the CR halo must be rigidity-dependent.

[4] O. Adriani et al. (CALET), Phys. Rev. Lett. **119**, 181101 (2017), 1712.01711
[5] O. Adriani et al., Phys. Rev. Lett. **120**, 261102 (2018), 1806.09728
[6] S. Abdollahi et al. (Fermi-LAT), Phys. Rev. **D95**, 082007 (2017), 1704.07195
[7] F. Aharonian et al. (H.E.S.S.), Phys. Rev. Lett. **101**, 261104 (2008), 0811.3894
[8] F. Aharonian et al. (H.E.S.S.), Astron. Astrophys. **508**, 561 (2009), 0905.0105
[9] A. Archer et al. (VERITAS), Phys. Rev. **D98**, 062004 (2018), 1808.10028
[10] A.K. Mallot, Ph.D. thesis, DESY (2017)
[11] M. Graziani (AMS), Cosmic Ray Transport and Energetic Radiations (CRATER 2018): Gran Sasso Science Institute, Italy, May 28, 2018 (2018)
[12] L. Bergstrom, T. Bringmann, J. Edsjo, Phys. Rev. **D78**, 103520 (2008), 0808.3725
[13] I. Cholis, L. Goodenough, D. Hooper, M. Simet, N. Weiner, Phys. Rev. **D80**, 123511 (2009), 0809.1683
[14] V. Barger, W.Y. Keung, D. Marfatia, G. Shaughnessy, Phys. Lett. **B672**, 141 (2009), 0809.0162
[15] M. Cirelli, A. Strumia, PoS **IDM2008**, 089 (2008), 0808.3867
[16] A.M. Atoyan, F.A. Aharonian, H.J. Völk, Phys. Rev. D **52**, 3265 (1995)
[17] A. Boulares, The Astrophysical Journal **342**, 807 (1989)
[18] S. Profumo, Central Eur. J. Phys. **10**, 1 (2011), 0812.4457
[19] D. Hooper, P. Blasi, P.D. Serpico, JCAP **0901**, 025 (2009), 0810.1527
[20] B. Katz, K. Blum, E. Waxman, Mon. Not. Roy. Astron. Soc. **405**, 1458 (2010), 0907.1686
[21] K. Blum, R. Sato, M. Takimoto, Phys. Rev. **D98**, 063022 (2018), 1709.04953
[22] F. Donato, M. Korsmeier, M. Di Mauro, Phys. Rev. **D96**, 043007 (2017), 1704.03663
[23] K. Blum, B. Katz, E. Waxman, Phys. Rev. Lett. **111**, 211101 (2013), 1305.1324
[24] K. Blum, R. Sato, E. Waxman (2017), 1709.06507
[25] A.W. Strong, I.V. Moskalenko, V.S. Ptuskin, Ann. Rev. Nucl. Part. Sci. **57**, 285 (2007), astro-ph/0701517
[26] W.R. Webber, A. Soutoul, The Astrophysical Journal **506**, 335 (1998)
[27] K. Blum, JCAP **1111**, 037 (2011), 1010.2836
[28] M. Aguilar et al. (AMS), Phys. Rev. Lett. **120**, 021101 (2018)
[29] J.J. Engelmann, P. Ferrando, A. Soutoul, P. Goret, E. Juliusson, Astrophys. J. **233**, 96 (1990)
[30] G.R. Blumenthal, R.J. Gould, Rev. Mod. Phys. **42**, 237 (1970)
[31] C.C. Popescu, R. Yang, R.J. Tuffs, G. Natale, M. Rushton, F. Aharonian, Mon. Not. Roy. Astron. Soc. **470**, 2539 (2017), 1705.06652
[32] T.A. Porter, G. Johannesson, I.V. Moskalenko, Astrophys. J. **846**, 67 (2017), 1708.00816
[33] R. Schlickeiser, J. Ruppel, New J. Phys. **12**, 033044 (2010), 0908.2183
[34] Y. Génolini et al., Phys. Rev. Lett. **119**, 241101 (2017), 1706.09812
[35] A. Reinert, M.W. Winkler, JCAP **1801**, 055 (2018), 1712.00002
[36] Y.S. Yoon et al., Astrophys. J. **728**, 122 (2011), 1102.2575
[37] H.P. Dembinski, R. Engel, A. Fedynitch, T. Gaisser, F. Riehn, T. Stanev, PoS **ICRC2017**, 533 (2018), 1711.11432